ORIGINAL RESEARCH

Increased Protein Tyrosine Phosphatase 1B (PTP1B) Activity and Cardiac Insulin Resistance Precede Mitochondrial and Contractile Dysfunction in Pressure-Overloaded Hearts

T. Dung Nguyen, MD;* Michael Schwarzer, PhD;* Andrea Schrepper, PhD; Paulo A. Amorim, MD; Daniel Blum, MSc; Claudia Hain, MD; Gloria Faerber, MD; Judith Haendeler, PhD; Joachim Altschmied, PhD; Torsten Doenst, MD

***Background*—**Insulin resistance in diabetes mellitus has been associated with mitochondrial dysfunction. Defects at the level of mitochondria are also characteristic of heart failure. We assessed changes in cardiac insulin response and mitochondrial function in a model of pressure overload-induced heart failure.

***Methods and Results*—**Rats underwent aortic banding to induce pressure overload. At 10 weeks, rats showed cardiac hypertrophy and pulmonary congestion, but left ventricular dilatation and systolic dysfunction were only evident after 20 weeks. This contractile impairment was accompanied by mitochondrial dysfunction as shown by markedly reduced state 3 respiration of isolated mitochondria. Aortic banding did not affect systemic insulin response. However, insulin-stimulated cardiac glucose uptake and glucose oxidation were significantly diminished at 10 and 20 weeks, which indicates cardiac insulin resistance starting before the onset of mitochondrial and contractile dysfunction. The impaired cardiac insulin action was related to a decrease in insulin-stimulated phosphorylation of insulin receptor β. Consistently, we found elevated activity of protein tyrosine phosphatase 1B (PTP1B) at 10 and 20 weeks, which may blunt insulin action by dephosphorylating insulin receptor β. PTP1B activity was also significantly increased in left ventricular samples of patients with systolic dysfunction undergoing aortic valve replacement because of aortic stenosis.

***Conclusions*—**Pressure overload causes cardiac insulin resistance that precedes and accompanies mitochondrial and systolic dysfunction. Activation of PTP1B in the heart is associated with heart failure in both rats and humans and may account for cardiac insulin resistance. PTP1B may be a potential target to modulate insulin sensitivity and contractile function in the failing heart. **(*J Am Heart Assoc*. 2018;7:e008865. DOI: 10.1161/JAHA.118.008865.)**

Key Words: heart failure • insulin action • insulin resistance • mitochondria • protein phosphatase

Heart failure (HF) is a global public health burden with an estimated prevalence of ≈ 40 million patients worldwide. Despite some significant achievements in pharmacological and surgical therapy, the prognosis of HF remains worse than that of most cancers.[1] There is a great need for improved understanding of mechanisms leading to heart failure, which are complex and manifold.

We and others have suggested a role for mitochondrial remodeling and dysfunction in HF.[2,3] However, the mechanisms contributing to mitochondrial defects in HF are unclear. In diabetes mellitus, mitochondrial dysfunction has been associated with insulin resistance. Studies have shown that impaired mitochondrial function may cause insulin resistance in skeletal muscle.[4] Notably, the reverse relationship may also exist, which applies particularly to the heart. For example, genetic deletion of cardiac insulin receptor accelerates mitochondrial dysfunction in myocardial infarction (MI) and diabetic cardiomyopathy.[5,6]

From the Department of Cardiothoracic Surgery, Jena University Hospital, Friedrich Schiller University Jena, Jena, Germany (T.D.N., M.S., A.S., P.A.A., D.B., G.F., T.D.); Department of General and Visceral Surgery, Klinikum Burgenlandkreis, Zeitz, Germany (C.H.); IUF-Leibniz Research Institute for Environmental Medicine, Duesseldorf, Germany (J.H., J.A.); Central Institute of Clinical Chemistry and Laboratory Medicine, University of Duesseldorf, Germany (J.H.).

Accompanying Figures S1 through S3 are available at http://jaha.ahajournals.org/content/7/13/e008865/DC1/embed/inline-supplementary-material-1.pdf

*Dr Nguyen and Dr Schwarzer contributed equally to this work.

Correspondence to: Torsten Doenst, MD, Department of Cardiothoracic Surgery, Jena University Hospital, Friedrich Schiller University Jena, Am Klinikum 1, 07747 Jena, Germany. E-mail: doenst@med.uni-jena.de

Received March 1, 2018; accepted March 22, 2018.

Clinical Perspective

What Is New?

- Insulin resistance has been associated with mitochondrial dysfunction in diabetes mellitus and cardiac disorders, but it is unclear which defect occurs first and may therefore provoke the other.
- We show that chronic pressure overload causes isolated cardiac insulin resistance that precedes and accompanies mitochondrial and systolic dysfunction.
- Furthermore, this cardiac insulin resistance correlates with an activation of the protein tyrosine phosphatase 1B (PTP1B) in the heart, which is associated with systolic dysfunction in both rats and humans.

What Are the Clinical Implications?

- The findings suggest a role for cardiac insulin signaling in the pathophysiology of heart failure.
- They also point to PTP1B as a potential target to modulate cardiac insulin sensitivity and contractile function in the failing heart.

In a model of MI-induced HF, we previously found cardiac insulin resistance (cIR) associated with altered mitochondrial gene expression.[7] This suggests a link among cardiac insulin signaling and mitochondrial and contractile function in HF. Nevertheless, it remains unclear which of those changes occurs first and may therefore affect the others.

The present study aimed to investigate changes in cardiac insulin response and mitochondrial function at different time points in the development of pressure overload-induced HF. We found that pressure overload causes cIR that precedes and accompanies mitochondrial and systolic dysfunction. This cIR correlates with an activation of protein tyrosine phosphatase 1B (PTP1B) in the heart, which is associated with systolic dysfunction in both rats and humans. The findings suggest a role for cIR in the pathophysiology of HF and point to PTP1B as a potential target to modulate cardiac insulin sensitivity and contractile function.

Methods

The data that support the findings of this study are available from the corresponding author upon reasonable request.

Animals

Male Sprague–Dawley rats were obtained from Charles River (Sulzfeld, Germany) and housed under a light/dark cycle of 12 hours at 21°C with free access to food and water. All animals received humane care, and the experimental protocols were approved by the Animal Welfare Committee of the University of Leipzig and the University of Jena (AZ: 24-9168.11TVV36/06; 02-055/10). In total, 354 animals were used for the experiments.

Collection of Human Left Ventricular Samples

All experiments were conducted according to the Declaration of Helsinki. The procedure was approved by the institutional review board (ethics committee) of the University of Leipzig (Approval No. 212-2007) and the University of Jena (Approval No. 3206-07/11). All patients had to give written informed consent before their participation.

Patients were preoperatively divided into 3 groups depending on their heart valve function as well as their left ventricular ejection fraction (EF). The control group (n=3) involves patients with normotrophic hearts, normal EF (>50%), and without relevant valve dysfunction undergoing elective replacement of the ascending aorta. The second group (n=5) includes patients undergoing elective replacement of the aortic valve because of aortic stenosis with normal EF (>50%). Patients in the third group (n=2) are similar to those in the second, except that EF was reduced (<40%). General exclusion criteria are significant heart valve diseases other than aortic valve stenosis, significant coronary artery disease, diabetes mellitus, chronic kidney disease, and cancer. Echocardiography was performed preoperatively according to current guidelines. EF was measured in the apical 4-chamber view using the biplane method of discs.

Left ventricular samples were obtained from the basal septum using a technique resembling Morrow's procedure under intraoperative transesophageal echocardiographic guidance. Samples were immediately frozen in liquid nitrogen and stored at −80°C for measurement of PTP1B activity.

Experimental Design

Rats were subjected to chronic pressure overload at 3 weeks of age and were followed for 20 weeks. Because of the nature of the experiments, repeated assessments in the same animals were not possible. Therefore, rats were divided into subsets and euthanized for experiments at 2, 10, and 20 weeks.

Induction of Pressure Overload

Our surgical protocol for the induction of hypertrophy and HF in rats has been described in detail earlier.[8] Briefly, 3-week-old rats were anesthetized and ventilated with room air during the operation. Following a partial sternotomy and removal of the thymus, a titanium clip was placed around the aortic arch

between the brachiocephalic trunk and the left carotid artery. The clip had a remaining opening of 0.35 mm, causing progressively increased afterload. Age-matched sham controls underwent the same procedure except for clip application.

Echocardiographic Assessments

We previously described this method in detail.[9] In brief, rats were examined in supine position with a 12-MHz phased array transducer (Agilent/Philipps, Amsterdam, The Netherlands). Two-dimensional short-axis views of the left ventricle at the level of the papillary muscle were obtained for standard M-mode assessment. EF was determined according to Teicholz. All values were averaged by 3 consecutive measurements.

Quantitative Real-Time PCR

Myocardial mRNA was isolated from frozen tissue samples using the Qiagen RNeasy mini kit (Qiagen, Hilden, Germany). Synthesis of cDNA was performed using the cDNA synthesis kit from Fermentas (Waltham, MA). TaqMan quantitative real-time reverse transcriptase polymerase chain reaction was performed using AmpliTaq Gold (Applied Biosystems, Foster City, CA) with the conditions suggested by the manufacturer on the ABI 7900 HT as previously described.[10] Forward and reverse primers were designed using the Universal Probe Library Assay Design Center. Results were normalized to the invariant transcript of the ribosomal protein, S29, as a housekeeping gene product.

Isolation of Mitochondria

Cardiac mitochondria were isolated according to Palmer et al,[11] except that a modified Chappell–Perry buffer (containing 100 mmol/L of KCl, 50 mmol/L of MOPS, 1 mmol/L of EGTA, 5 mmol/L of $MgSO_4 \cdot 7H_2O$, and 1 mmol/L of ATP; pH 7.4, 4°C) was used. Mitochondria were harvested following treatment of the homogenate with trypsin (5 mg/g of heart weight) for 10 minutes at 4°C. Mitochondrial protein concentration was determined by the Bradford method using BSA as a standard.

Measurement of Mitochondrial Respiratory Capacity

Oxygen consumption rate of isolated mitochondria was measured using a Clark-type oxygen electrode (Strathkelvin) at 25°C. Mitochondria were incubated in a solution consisting of 80 mmol/L of KCl, 50 mmol/L of MOPS, 1 mmol/L of EGTA, 5 mmol/L of KH_2PO_4, and 1 mg/mL of fatty acid–free BSA at pH 7.4. Rate of oxidative phosphorylation was measured using glutamate, pyruvate and malate, and palmitoylcarnitine and malate as substrates and ADP as stimulus. ADP-stimulated oxygen consumption (state 3) in the respiratory chamber was determined and normalized to mitochondrial protein content as previously described.[12]

Hyperinsulinemic-Euglycemic Clamp

After an overnight fast, rats were anesthetized by intramuscular injection of a combination of midazolam hydrochloride, medetomidin hydrochloride, and fentanyl (2, 0.15, and 0.005 mg/kg). A catheter (HelixMark; Standard Silicone Tubing) was inserted into the right internal jugular vein and advanced to the superior vena cava. The proximal of the catheter was then connected to a syringe pump (TSE Systems, Bad Homburg vor der Höhe, Germany). After a bolus (1.6 μCi) injection of D-[3-^{3}H] glucose (PerkinElmer, Waltham, MA), the tracer was infused continuously at a rate of 0.02 μCi/min. At 80 minutes, 50 μL of blood were obtained from the tail vein for basal values and insulin (Eli Lilly and Company, Indianapolis, IN) was infused at a rate of 30 mU/kg/min. Blood glucose levels were determined every 5 minutes (Accu-Chek Performa; Roche Diabetes Care, Castle Hill, NSW, Australia). Physiological blood glucose levels (between 5.3 and 5.7 mmol/L) were maintained by varying the infusion rate of a 40% glucose solution (B. Braun, Melsungen, Germany). When steady state was established (glucose measurements were constant for at least 15 minutes at a fixed glucose infusion rate), 50 μL of blood were anew sampled and a bolus (2 μCi) of 2-deoxy-D-[1-^{14}C] glucose (PerkinElmer) was manually applied. At 5, 10, 15, 25, 35, and 45 minutes after the injection of the 2-deoxy-D-[1-^{14}C] glucose, blood samples were collected. At the end of the experiment, rats were euthanized by cervical dislocation for organ harvesting.

Plasma [3-^{3}H] glucose radioactivity of basal and steady-state samples was determined after deproteinization with 0.3 mol/L of $Ba(OH)_2$ and 0.3 mol/L of $ZnSO_4$ and also after removal of ^3H_2O by evaporation using a liquid scintillation counter (Beckman Coulter, Brea, CA). Plasma deoxy-[1-^{14}C] glucose radioactivity was measured directly in the liquid scintillation counter. Tissue lysates were processed through ion exchange chromatography columns (BioRad AG1-X8 formate resin; Bio-Rad Laboratories, Hercules, CA) to separate 2-deoxy-D-[1-^{14}C] glucose from 2-deoxy-D-[1-^{14}C] glucose-6-phosphate.

Isolated Working Heart Perfusion

We described the technique of the isolated working heart perfusion in detail before.[13] Rat hearts were perfused in the working mode with both glucose (5 mmol/L) and oleate

(0.4 mmol/L) as substrates. All experiments were carried out with a preload of 15 cm of H_2O and an afterload of 100 cm of H_2O. After stabilization, hearts were perfused for 30 minutes. Subsequently, insulin (0.5 mU/mL) was added and hearts were perfused for further 30 minutes. Every 5 minutes, a sample of coronary effluent was withdrawn for the measurement of glucose oxidation determined as the production of $^{14}CO_2$ from [U-^{14}C]-glucose.

Immunoblotting

We used immunoprecipitation for the assessment of the insulin receptor β subunit (IRβ). Total heart lysates were incubated with 1 μg of anti-IRβ antibody (C-19; Santa Cruz Biotechnology, Santa Cruz, CA) overnight at 4°C. Protein G/agarose beads were added for 3 hours and immunoprecipitates were washed 3 times in lysis buffer, eluted in 2× SDS buffer and subjected to SDS-PAGE.

After SDS-PAGE electrophoresis, proteins were blotted to a PVDF membrane using a semidry electrophoretic apparatus and incubated with primary and secondary antibodies. Bands were visualized by chemiluminescence and semiquantified using AIDA Image Analyzer software. Total protein stains with naphthol blue black were used as loading controls. Antibodies against protein kinase B (Akt), Phospho-Akt (Ser473), insulin receptor substrate 1 (IRS1), Phospho-IRS1 (Ser636/639) were obtained from Cell Signaling Technology (Danvers, MA). Antiphosphotyrosine antibody was from Upstate Biotechnology, (Lake Placid, NY).

Immunoblotting of PTP1B was performed in Duesseldorf using a similar standard procedure. Anti-PTP1B antibody was obtained from ECM Biosciences (Versailles, KY). GAPDH (Abcam, Cambridge, MA) was used as loading controls. Semiquantitative analyses were performed on scanned X-ray films using ImageJ (NIH, Bethesda, MD) 1.42q.

In Vivo Insulin Stimulation

To assess insulin-stimulated phosphorylation of IRβ in the heart, rats were anesthetized with sodium pentobarbital. Insulin (0.5 mU/g) was injected into the inferior vena cava. After 5 minutes, hearts were rapidly explanted. Residual blood and the atria were removed, and ventricular samples were immediately frozen in liquid nitrogen and stored at −80°C.

Measurement of PTP1B Activity

PTP1B activity was measured in rat and patient heart tissue with p-nitrophenyl phosphate as substrate according to Montalibet et al.[14] In brief, heart tissue (30–40 mg) was homogenated in lysis buffer (50 mmol/L of Bis-Tris, 2 mmol/L of EDTA, 0.1 mmol/L of PMSF, 5 mmol/L of DTT, 0.5% Triton X-100, and 20% glycerol), allowed to dissolve on ice, and protein content was determined. Dilution buffer (50 mmol/L of Bis-Tris, 2 mmol/L of EDTA, 5 mmol/L of DTT, and 20% glycerol) was prepared freshly, samples were diluted to a final concentration of 0.2 μg/μL and assay was performed in triplicates. The reaction was started by addition of 175 μL of assay buffer (50 mmol/L of Bis-Tris, 2 mmol/L of EDTA, 5 mmol/L of DTT, 0.01% Triton X-100, and 15 mmol/L of p-nitrophenyl phosphate) and allowed to run for 10 minutes. Reaction was stopped by addition of 20 μL of 10 mol/L of NaOH, and absorption was measured at 405 nm 3 minutes thereafter.

Statistical Analysis

We used the 2-tailed Student *t* test for the analysis of Western blot data, 1-way ANOVA for PTP1B activity in patients, and 2-way ANOVA with interaction analysis for all other data. The Holm–Sidak method was applied for pairwise comparisons. Data are plotted using SigmaPlot 13.0. All statistical tests were performed using SigmaStat 4.0. Statistical significance was assumed if $P<0.05$.

Results

Although comparisons between time points were also made by the analyses, we will focus on the differences between aortic-banded groups and their time-matched controls in describing the results.

Aortic Banding Induces Left Ventricular Dilatation and Systolic Dysfunction at 20 Weeks

Aortic banding (AoB) resulted in marked cardiac hypertrophy as early as 2 weeks as shown by increased left ventricular mass index and increased heart-to-body weight ratio (Table 1; Figure 1A). At 10 weeks, whereas the lung-to-body weight index was significantly higher in the AoB group, left ventricular end diastolic diameter and left ventricular EF remained unchanged (Figure 1B through 1D). This stage represents HF with preserved EF, which we described in detail previously.[9,15] At 20 weeks, left ventricular end diastolic diameter was increased and EF was decreased (Figure 1C and 1D), indicating left ventricular dilatation and systolic dysfunction, respectively.

Aortic Banding Results in Mitochondrial Dysfunction at 20 Weeks

Mitochondrial biogenesis and function are regulated by a set of nuclear-encoded factors. The mitochondrial transcription

Table 1. Selected Basic and Echocardiographic Parameters

	2 Weeks		10 Weeks		20 Weeks	
	Control	AoB	Control	AoB	Control	AoB
Body weight, g	133.9±7.2	113.8±6.1*	346.7±5.5[a]	328.8±5.7*[a]	428.7±6.3[ab]	418.8±6.5[ab]
Heart weight, mg	617.3±121.4	631.9±102.6	1337.9±93.1[a]	2589.9±96.0*[a]	1293.6±106.5[a]	2794.1±110.8*[a]
Lung weight, mg	750.8±395.0	803.1±255.0	1619.5±266.3	3910.2±228.0*[a]	1698.6±228.0	3976.3±279.3*[a]
Heart rate, bpm	295.1±9.3	282.3±8.9	231.1±8.6[a]	255.8±10.2	229.3±14.4[a]	234.4±12.2[a]
LVMI, g/kg	2.7±0.3	4.3±0.2*	2.5±0.2	4.3±0.3*	2.6±0.4	5.7±0.3*[ab]

Data are least squares mean±SEM, n=5 to 17 per group. Statistical analysis: 2-way ANOVA with the Holm–Sidak method for pairwise comparisons. AoB indicates aortic banding; LVMI, left ventricular mass index.
*Significantly different vs control.
Significantly different vs [a]2 weeks, vs [b]10 weeks (within control or AoB).

factor A (TFAM), nuclear respiratory factors (NRF)1 and 2, estrogen-related receptor α (ERRα), and the peroxisome proliferator-activated receptor α (PPARα) directly promote the transcription of mitochondrial proteins. The activities of these transcription factors are coordinately regulated by the peroxisome proliferator-activated receptor gamma coactivators PGC-1α and PGC-1β, which have overlapping targets and may support each other.[16]

Figure 2A shows changes in mRNA expression of genes regulating mitochondrial biogenesis. At 2 weeks, mRNA levels of PGC-1β were significantly decreased. At 10 weeks, significant reductions were found for PGC-1α, TFAM, and ERRα. At

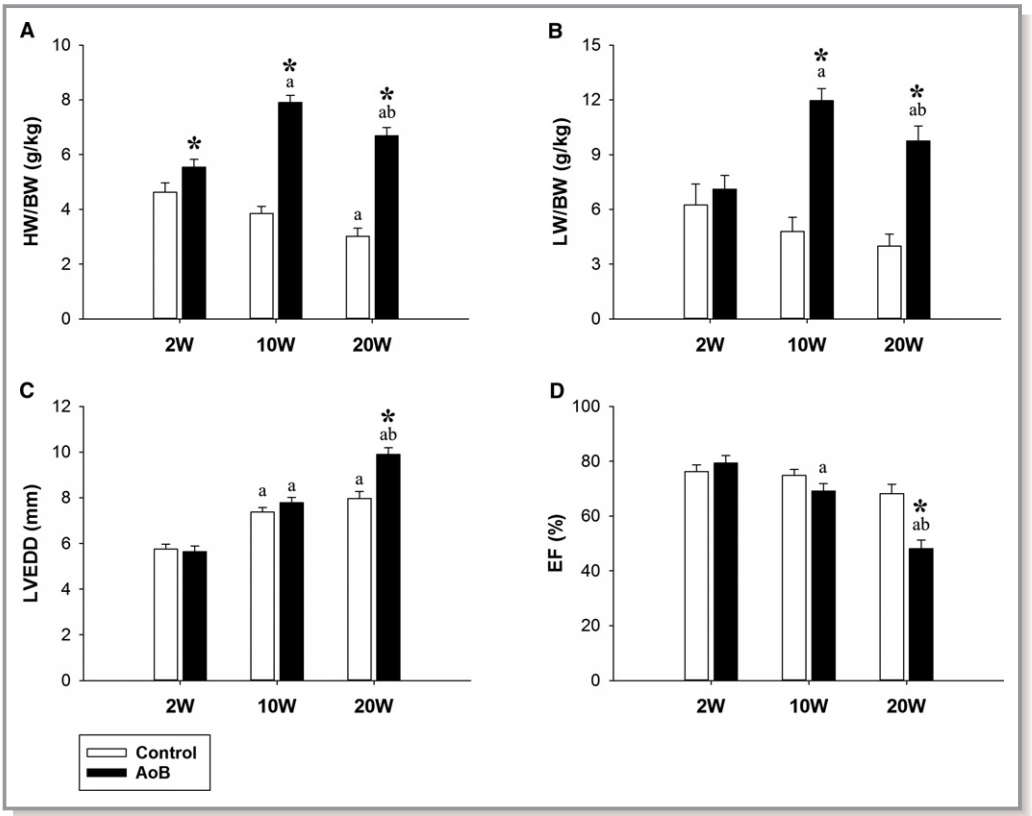

Figure 1. Cardiopulmonary morphological and functional changes at 2, 10, and 20 weeks after aortic banding. Changes in heart-to-body weight index (HW/BW; n=12–17) (A). Changes in lung-to-body weight index (LW/BW; n=5–15) (B). Changes in left ventricular end diastolic dimension (LVEDD; n=6–14) (C). Changes in left ventricular ejection fraction (EF; n=6–13) (D). Data are least squares mean±SEM. Statistical analysis: 2-way ANOVA with the Holm–Sidak method for pairwise comparisons. Significantly different vs control: *. Significantly different vs 2 weeks: a, vs 10 weeks: b (within control or AoB). AoB indicates aortic banding.

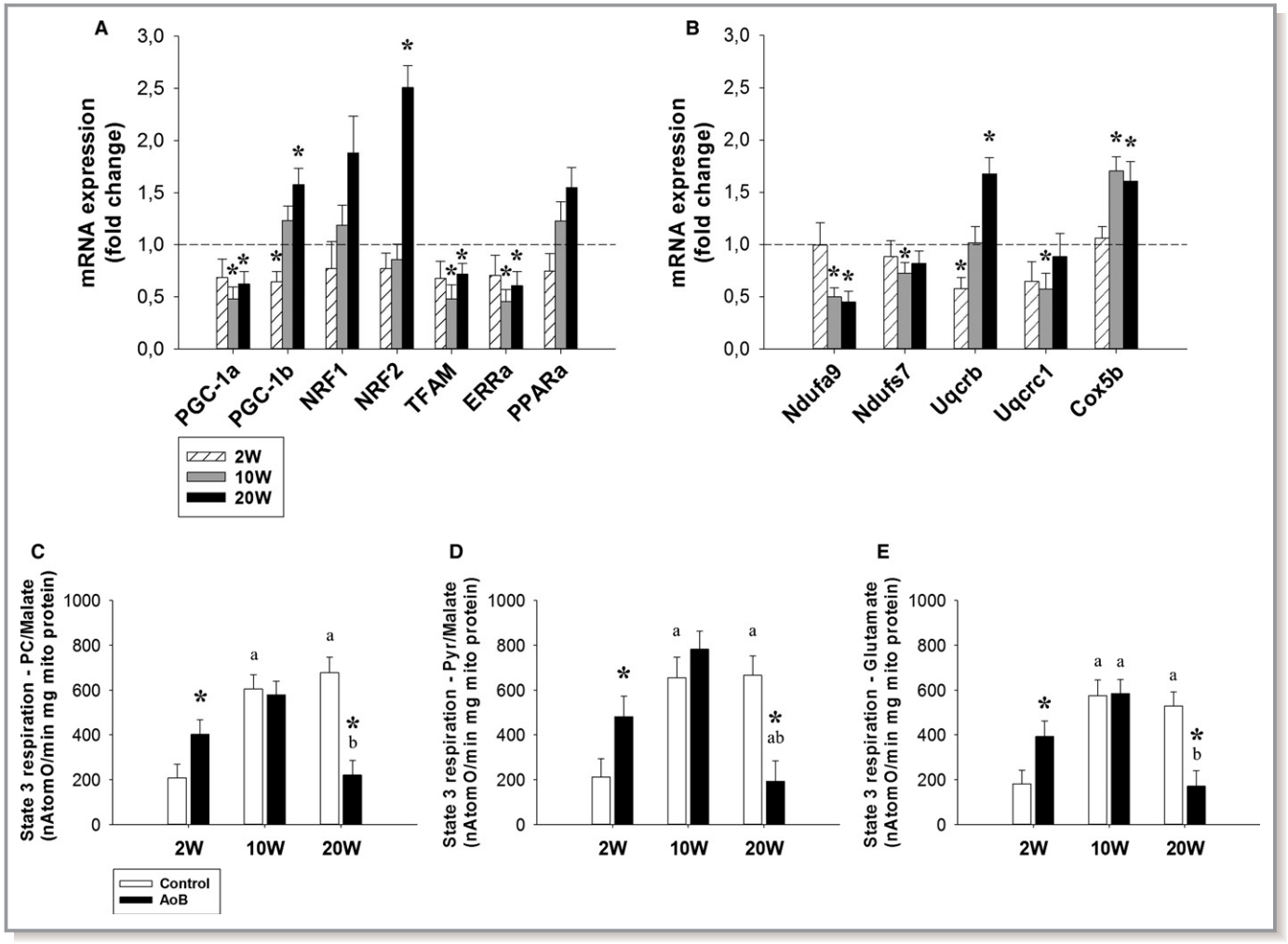

Figure 2. Cardiac mitochondrial gene expression and respiratory capacity at 2, 10, and 20 weeks after aortic banding. Changes in mRNA expression of genes regulating mitochondrial biogenesis and function (n=4–12) (A). Changes in mRNA expression of mitochondrial respiratory chain complex subunits (n=4–12) (B). Asterisks in (A and B) indicate significant differences compared with time-matched controls represented by the reference line. State 3 respiration of isolated mitochondria with palmitoylcarnitine and malate as substrates (n=7–9) (C). State 3 respiration of isolated mitochondria with pyruvate and malate as substrates (n=7–9) (D). State 3 respiration of isolated mitochondria with glutamate as substrate (n=7–9) (E). Data are least squares mean±SEM. Statistical analysis: 2-way ANOVA with the Holm–Sidak method for pairwise comparisons. Significantly different vs control: *. Significantly different vs 2 weeks: a, vs 10 weeks: b (within control or AoB). AoB indicates aortic banding.

20 weeks, whereas PGC-1α, TFAM, and ERRα remained lower than controls, expressions of PGC-1β and NRF2 were significantly elevated, which may imply a compensatory regulation. Interestingly, expression of PPARα was unaffected by AoB at all 3 time points.

Next, we assessed whether the observed changes in mitochondrial transcriptional control influenced mRNA expression of mitochondrial structural proteins. Ndufa9 and Ndufs7 are subunits of complex I, Uqcrb and Uqcrc1 are subunits of complex III, and Cox5b is a subunit of IV. Figure 2B shows diverse changes in these complexes. For example, expression of Ndufa9 was reduced at 10 and 20 weeks, but expression of Cox5b was elevated at these time points. Taken together, pressure overload significantly affected mRNA expression of mitochondrial regulators and complex proteins. Decreases in some proteins coincide with increases in others, which possibly imply compensatory responses.

See also Figures S1 and S2 for individual control groups and complete results of the ANOVA analyses.

Whereas mitochondria-related genes showed diverse expression patterns, measurement of mitochondrial respiratory capacity revealed a consistent response of mitochondrial function to pressure overload for all 3 substrates. State 3 respiration was initially increased at 2 weeks, unchanged at 10 weeks, and, finally, decreased at 20 weeks (Figure 2C

Table 2. State 4 Respiration and Respiratory Control Index of Isolated Mitochondria

	2 Weeks		10 Weeks		20 Weeks	
	Control	AoB	Control	AoB	Control	AoB
PC/malate						
State 4	113.8±9.3	96.1±9.9	118.3±9.9	91.9±9.3	93.1±10.7	92.5±9.9
RCI	1.9±0.4	4.2±0.4*	5.0±0.4[a]	6.4±0.4*[a]	7.1±0.5[ab]	2.4±0.4*[ab]
Pyruvate/malate						
State 4	115.5±16.3	105.4±18.5	119.0±18.5	129.9±16.3	146.9±17.3	95.3±18.5
RCI	1.9±0.5	4.5±0.6*	5.4±0.6[a]	6.3±0.5[a]	5.0±0.5[a]	2.0±0.6*[ab]
Glutamate						
State 4	90.1±9.5	84.9±10.7	103.0±10.7	85.9±9.5	95.8±9.5	72.9±10.7
RCI	2.1±0.5	4.7±0.6*	5.7±0.6[a]	6.9±0.5[a]	5.7±0.5[a]	2.4±0.6*[ab]

The unit of state 4 respiration: nAtomO/min mg mitochondrial protein. Data are least squares mean±SEM, n=7 to 9 per group. Statistical analysis: 2-way ANOVA with the Holm–Sidak method for pairwise comparisons. AoB indicates aortic banding; PC, palmitoylcarnitine; RCI, respiratory control index.
*Significantly different vs control.
Significantly different vs [a]2 weeks, vs [b]10 weeks (within control or AoB).

through 2E). The establishment of mitochondrial dysfunction correlated with, and may therefore contribute to, systolic dysfunction at 20 weeks.

Table 2 shows state 4 respiration and the respiratory control index. In general, state 4 respiration was not affected by aortic banding. In contrast, respiratory control index showed a similar pattern to state 3 respiration. At 2 weeks, respiratory control index was significantly increased with all three substrates. At 10 weeks, a significant but smaller increase was found with palmitoylcarnitine/malate. At 20 weeks, respiratory control index was consistently decreased irrespective of the substrate used.

AoB Causes Isolated cIR Starting at 10 Weeks

Human studies have associated HF with diabetes mellitus,[17] and diabetes mellitus itself may affect cardiac insulin signaling.[18] Therefore, we assessed both systemic and cardiac insulin response using hyperinsulinemic-euglycemic clamp. We found no differences in insulin-stimulated glucose infusion rate at all 3 time points (Figure 3A). Despite normal systemic insulin response, insulin-stimulated cardiac glucose uptake in the AoB group was significantly reduced at 10 and 20 weeks (Figure 3B). Consistently, isolated working heart perfusion showed decreased insulin-stimulated glucose oxidation (Figure 3C) and lower insulin-induced gain in glucose oxidation (ie, the difference between insulin-stimulated glucose oxidation and basal glucose oxidation) at 10 and 20 weeks compared with controls (Figure 3D). Taken together, although systemic insulin action was normal, we found a marked perturbation of cardiac insulin responsiveness that started at 10 weeks and persisted until 20 weeks. Therefore, this cIR developed before the onset of, and subsequently accompanied, mitochondrial and systolic dysfunction.

Alterations in Cardiac Insulin Signaling

To elucidate the mechanisms leading to cIR, we assessed changes in insulin signaling cascade in the heart. The serine/threonine kinase, Akt, also known as protein kinase B, plays a central role in insulin-induced glucose uptake. Furthermore, impaired Akt signaling is characteristic of insulin resistance in diabetes mellitus.[19] Figure 4A shows changes in Akt signaling in our model. At 2 weeks, although total Akt was reduced, phosphorylated Akt was significantly increased up to 3-fold. At 10 weeks, both total and phosphorylated Akt were clearly higher compared with controls. At 20 weeks, only total Akt was significantly elevated. Overall, we found no impairment, but rather an activation of Akt signaling particularly at 2 and 10 weeks. Thus, Akt is unlikely involved in cIR in our model.

IRS1 acts upstream of Akt. Dysregulation of IRS1 has been considered a key mechanism of insulin resistance in diabetes mellitus.[20] In addition, recent findings have also linked IRS1 to the regulation of mitochondrial function in the heart.[21] We therefore assessed changes at the level of IRS1. Figure 4B demonstrates that the total level of IRS1 was unaffected by AoB. However, the regulation of IRS1 activity is highly complex and may occur through phosphorylation at more than 10 serine/threonine residues.[20] We chose to assess the phosphorylation at Ser636/639 because increased phosphorylation at this site has repeatedly been shown to inhibit insulin signaling in diabetes mellitus.[22,23] However, IRS1 phosphorylation at Ser636/639 was normal as shown by

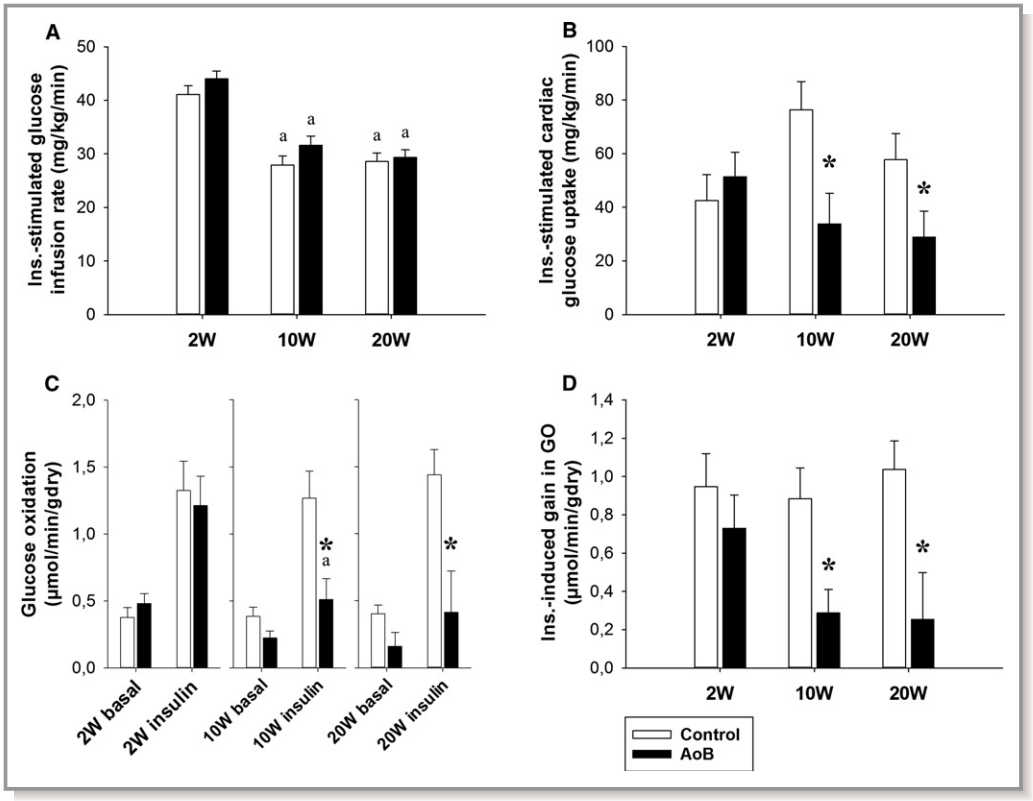

Figure 3. Changes in insulin-stimulated systemic and cardiac glucose utilization at 2, 10, and 20 weeks after aortic banding. Insulin-stimulated glucose infusion rate (n=6–9) (A). Insulin-stimulated cardiac glucose uptake (n=5–9) (B). Basal and insulin-stimulated myocardial glucose oxidation (n=3–12) (C). Insulin-induced gain in myocardial glucose oxidation (n=3–12) (D). Data are least squares mean±SEM. Statistical analysis: 2-way ANOVA with the Holm–Sidak method for pairwise comparisons. Significantly different vs control: *. Significantly different vs 2 weeks: a (within control or AoB).

unchanged ratio of P-IRS1/total IRS1 at all 3 time points (Figure 4B).

See also Figure S3 for individual control groups and representative blots.

Next, we assessed the regulation of the insulin receptor. We found no changes in protein levels of IRβ (Figure 4C). Similarly, tyrosine phosphorylation of IRβ was also unaffected by AoB in the basal state (Figure 4D). However, under insulin stimulation, tyrosine phosphorylation of IRβ tended to increase at 2 weeks, was unchanged at 10 weeks, and, finally, decreased at 20 weeks (Figure 4E). These findings imply a mechanism that affects the phosphorylation of the IRβ only if the receptor is activated.

Cardiac PTP1B Activity Is Increased in Rats and Humans and Associated With Systolic Dysfunction

By binding to the activated insulin receptor and dephosphorylating it, PTP1B acts as a negative regulator of insulin signaling.[24,25] Consistent with the finding that insulin-stimulated tyrosine phosphorylation of IRβ was decreased at 20 weeks (Figure 4E), protein expression of PTP1B was significantly elevated at 20 weeks (Figure 5A). Furthermore, the activity of PTP1B in pressure-overloaded rat hearts was unchanged at 2 weeks, but significantly increased at 10 and 20 weeks (Figure 5B), which exactly reflects the dynamics of cIR described above (Figure 3B through 3D).

To test the clinical relevance of our findings, we measured left ventricular PTP1B activity in patients undergoing elective cardiac surgery. In the control group (n=3 males, age=64±9 years), the patients showed normal systolic function (EF=62.3±1.2%) in the absence of valvular heart disease. The patients in the second group (n=3 females+2 males, age=64±5 years) displayed significant aortic stenosis, but normal systolic function (EF=68.6±1.1%). The third group (n=2 males, age=68±8 years) involves patients with both significant aortic stenosis and markedly reduced ejection fraction (EF=35.0±3.0%). Figure 6 shows that PTP1B activity in patients with reduced EF was significantly increased compared with those with normal EF, irrespective of aortic stenosis. In accord with the findings in rats, the results in

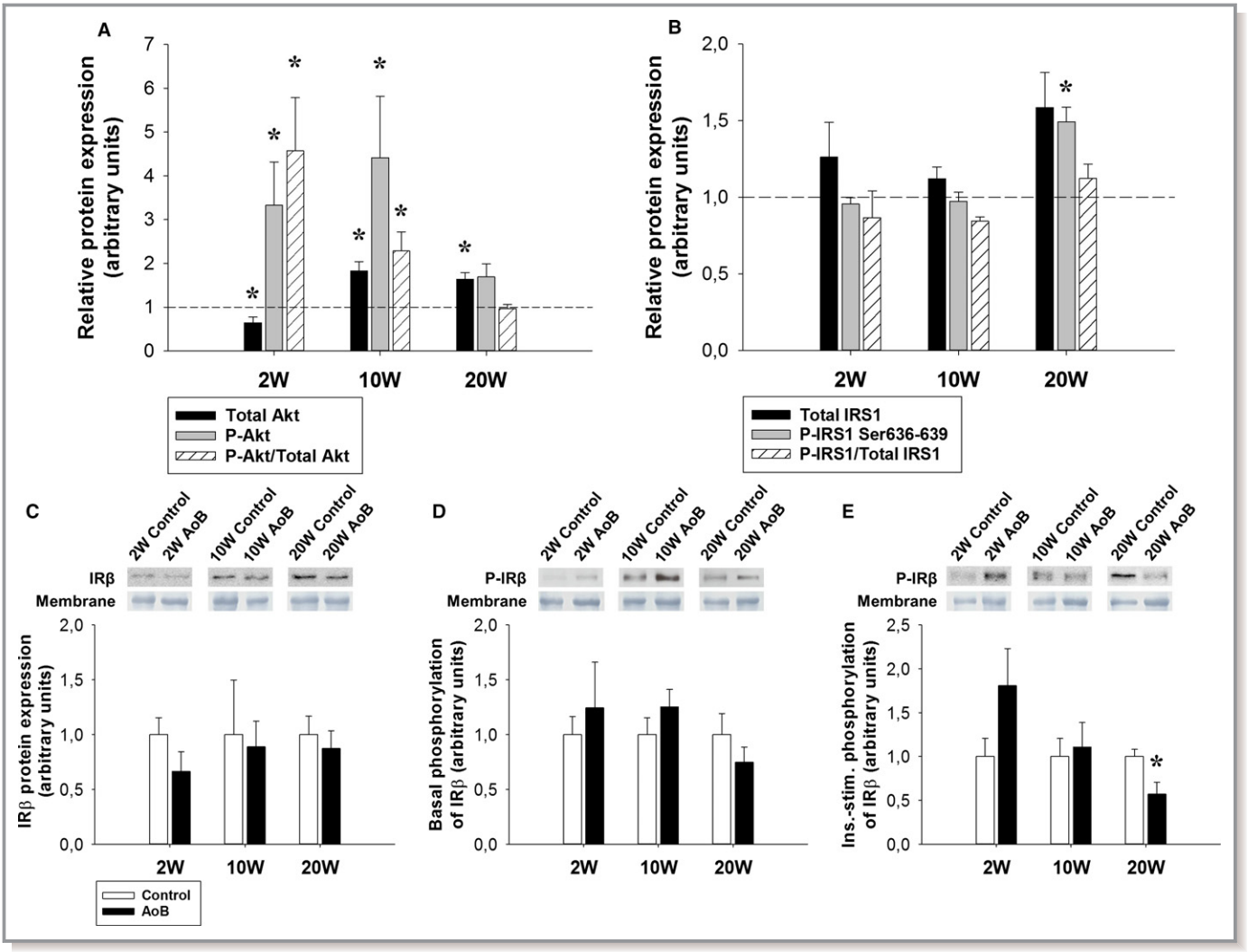

Figure 4. Regulation of insulin signaling mediators in the heart at 2, 10, and 20 weeks after aortic banding. Protein expression and serine phosphorylation of Akt (n=5–7) (A). Protein expression and phosphorylation at Ser636/639 of IRS1 (n=4–7) (B). Asterisks in (A) and (B) indicate significant differences compared with time-matched controls represented by the reference line. Protein expression of the insulin receptor β (n=5–8) (C). Basal phosphorylation of the insulin receptor (IR) β (n=6) (D). Insulin-stimulated phosphorylation of the insulin receptor β (n=5–8) (E). Data are mean±SEM. Statistical analysis: Student *t* test. Significantly different vs control. Akt indicates protein kinase B; AoB, aortic banding; IRS1, insulin receptor substrate-1.

humans also support a link between elevated PTP1B activity and systolic dysfunction.

Discussion

Studies in genetic models have shown that impaired cardiac insulin signaling has an adverse impact on mitochondrial and contractile function.[5,6] However, whether cardiac insulin action is affected in clinically relevant models of HF is unclear. In the present study, we demonstrate the presence of cIR in a well-established model of HF. Notably, we found that cIR developed before the onset of, and subsequently accompanied, mitochondrial and contractile dysfunction. This cIR was not related to systemic insulin sensitivity, but may potentially result from increased PTP1B activity in the heart. Importantly, we show, for the first time, that systolic dysfunction in humans is associated with increased left ventricular PTP1B activity. The findings suggest a role for cIR in the pathophysiology of HF and point to PTP1B as a potential target to modulate mitochondrial and cardiac function.

In the literature, there is a growing body of evidence linking PTP1B to HF. In mice with MI, Gomez et al showed that genetic deletion of PTP1B improved cardiac output without reducing infarct size. They attributed the protective effects to enhanced endothelial nitric oxide synthase signaling and endothelial function.[26] Recently, Gogiraju et al demonstrated in mice with pressure overload that endothelial deletion of PTP1B preserved systolic function, which was associated with

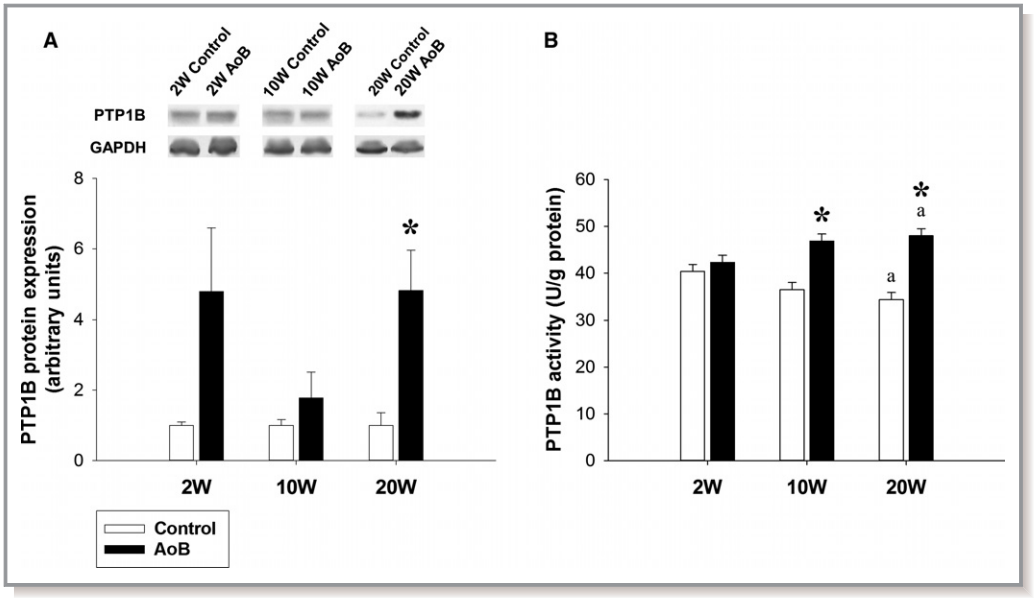

Figure 5. Protein expression and activity of PTP1B in the heart at 2, 10, and 20 weeks after aortic banding. Protein expression of PTP1B (n=3) (A). In A: Data are mean±SEM. Statistical analysis: Student *t* test. PTP1B activity (n=6) (B). In (B): Data are least squares mean±SEM. Statistical analysis: 2-way ANOVA with the Holm–Sidak method for pairwise comparisons. Significantly different vs control: *. Significantly different vs 2 weeks: a (within control or AoB). AoB indicates aortic banding; PTP1B, protein tyrosine phosphatase 1B.

improved angiogenesis.[27] Interestingly, we previously showed that cIR is characteristic of MI.[7] Here, we also found a strong correlation between cIR and pressure overload-induced HF.

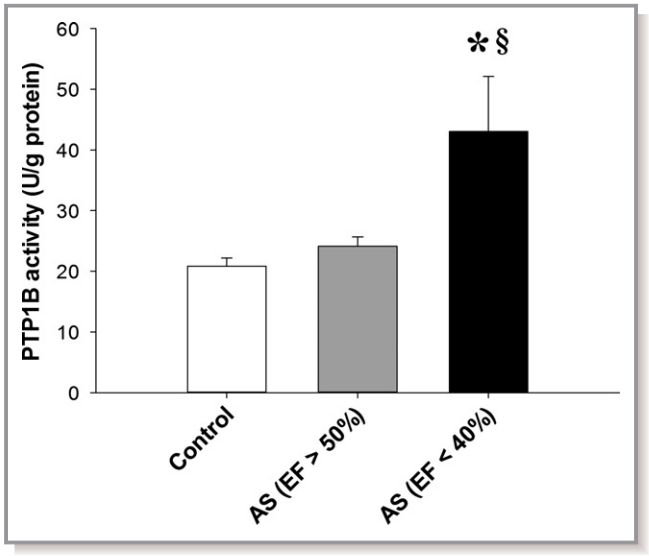

Figure 6. Left ventricular PTP1B activity in humans with normal and reduced ejection fraction. n=3 in control, n=5 in AS with normal ejection fraction (EF >50%), n=2 in AS with reduced ejection fraction (EF <40%). Data are mean±SEM. Statistical analysis: 1-way ANOVA. Significantly different vs control: *, vs AS (EF >50%): §. AoB indicates aortic banding; AS, aortic stenosis; PTP1B, protein tyrosine phosphatase 1B.

Therefore, although the studies by Gomez et al and Gogiraju et al did not assess cardiac insulin response, it is also possible that enhanced cardiac insulin sensitivity contributed to the favorable effects of PTP1B inhibition. Taken together, studies on the role of PTP1B in cardiac disorders have thus far focused on endothelial function and angiogenesis. By linking PTP1B to cardiac insulin action and contractile function, our findings are in line with previous results, but also reveal a novel mechanism potentially accounting for the benefits of PTP1B inhibition.

Impaired insulin signaling has been associated with mitochondrial dysfunction in diabetes mellitus and cardiac disorders.[4,28] However, it remains a matter of debate whether mitochondrial dysfunction results in insulin resistance or vice versa.[29,30] By showing, for the first time, that cIR accompanies, but develops before mitochondrial dysfunction, our results may support a role for cIR in the pathophysiology of HF.

In fact, there is accumulating evidence suggesting insulin signaling as a key regulator of mitochondrial function. In human skeletal muscle, insulin stimulates the synthesis of mitochondrial proteins and mitochondrial ATP production.[31] Similarly, perfusing rat hearts with insulin increases mitochondrial protein synthesis and respiration.[32] Insulin plays a crucial role for mitochondrial function given that impaired insulin signaling alone is capable of inducing mitochondrial defects. For example, disrupting the insulin receptor in

myotubes impairs PGC-1α signaling and mitochondrial bioenergetics.[33] In the heart, deletion of the insulin receptor promotes oxidative stress and diminishes mitochondrial respiratory capacity.[34] Consistently, cardiomyocyte-specific loss of the insulin receptor accelerates cardiac mitochondrial dysfunction and thereby worsens left ventricular function and survival in mice with MI.[5] Therefore, it is reasonable to postulate that the development of cIR in pressure-overloaded hearts was an important trigger of mitochondrial dysfunction. The specific mechanisms how cIR affects mitochondria are still unclear. However, because insulin resistance may impair PGC-1α signaling[33] and the dynamics of PGC-1α gene expression (Figure 2A) resemble that of cardiac insulin sensitivity, we assume that PGC-1α may be involved.

There are further interesting aspects of our results that need to be discussed. First, we found a consistent biphasic response of state 3 respiration. In contrast, changes in mRNA expression of mitochondrial complex proteins and regulators are divergent and do not reveal a specific pattern. The mechanisms accounting for the discrepancies between gene expression and mitochondrial respiration remain undefined and may be interesting for future investigations.

Second, we found that Akt phosphorylation was increased at 2 and 10 weeks, but unchanged at 20 weeks (Figure 4A), which was independent of cIR. Although Akt plays a key role in mediating insulin effects on glucose metabolism, Akt is also involved in hypertrophic signaling.[35,36] Because the changes in Akt phosphorylation are in concert with those in heart weight (rapid gain from 2 to 10 weeks; Table 1), Akt appears to be primarily regulated by hypertrophic signals in our model. Of note, recent evidence suggests that chronic activation of Akt may affect mitochondrial biogenesis and function.[37] Thus, it is possible that the prolonged activation of Akt also contributed to mitochondrial dysfunction.

Third, the fact that insulin-stimulated tyrosine phosphorylation of IRβ was normal at 10 weeks (Figure 4E), but PTP1B activity was increased (Figure 5B) and cIR was already manifest at this time point (Figure 3B through 3D), suggests additional targets for PTP1B downstream of the insulin receptor. Given that PTP1B may also dephosphorylate IRS1,[38] we speculate that IRS1 phosphorylation may be affected by PTP1B leading to cIR at 10 weeks. In this study, we were not able to verify this possibility because of the complex regulation of IRS1, which includes at least 10 phosphorylation sites.[20]

Fourth, we could only include 2 patients with reduced EF for the measurement of cardiac PTP1B activity. Although significance was reached attributable to the great differences between groups, the small sample size certainly results in a large confidence interval.

Finally, although we provide evidence supporting a role for PTP1B in cIR and HF, a definitive mechanistic link remains to be validated. For this purpose, specific manipulations of PTP1B activity and insulin sensitivity in pressure-overloaded hearts would be necessary.

Sources of Funding

This study was mainly supported by grants from the DFG (Deutsche Forschungsgemeinschaft) to Doenst, and partly by a grant from the DFG (SFB1116 TP A04) to Haendeler and Altschmied.

Disclosures

None.

References

1. Braunwald E. The war against heart failure: the lancet lecture. *Lancet*. 2015;385:812–824.
2. Bugger H, Schwarzer M, Chen D, Schrepper A, Amorim PA, Schoepe M, Nguyen TD, Mohr FW, Khalimonchuk O, Weimer BC, Doenst T. Proteomic remodelling of mitochondrial oxidative pathways in pressure overload-induced heart failure. *Cardiovasc Res*. 2010;85:376–384.
3. Dai DF, Hsieh EJ, Liu Y, Chen T, Beyer RP, Chin MT, MacCoss MJ, Rabinovitch PS. Mitochondrial proteome remodelling in pressure overload-induced heart failure: the role of mitochondrial oxidative stress. *Cardiovasc Res*. 2012;93:79–88.
4. Montgomery MK, Turner N. Mitochondrial dysfunction and insulin resistance: an update. *Endocr Connect*. 2015;4:R1–R15.
5. Sena S, Hu P, Zhang D, Wang X, Wayment B, Olsen C, Avelar E, Abel ED, Litwin SE. Impaired insulin signaling accelerates cardiac mitochondrial dysfunction after myocardial infarction. *J Mol Cell Cardiol*. 2009;46:910–918.
6. Bugger H, Riehle C, Jaishy B, Wende AR, Tuinei J, Chen D, Soto J, Pires KM, Boudina S, Theobald HA, Luptak I, Wayment B, Wang X, Litwin SE, Weimer BC, Abel ED. Genetic loss of insulin receptors worsens cardiac efficiency in diabetes. *J Mol Cell Cardiol*. 2012;52:1019–1026.
7. Amorim PA, Nguyen TD, Shingu Y, Schwarzer M, Mohr FW, Schrepper A, Doenst T. Myocardial infarction in rats causes partial impairment in insulin response associated with reduced fatty acid oxidation and mitochondrial gene expression. *J Thorac Cardiovasc Surg*. 2010;140:1160–1167.
8. Zaha V, Grohmann J, Gobel H, Geibel A, Beyersdorf F, Doenst T. Experimental model for heart failure in rats—induction and diagnosis. *Thorac Cardiovasc Surg*. 2003;51:211–215.
9. Shingu Y, Amorim PA, Nguyen TD, Osterholt M, Schwarzer M, Doenst T. Echocardiography alone allows the determination of heart failure stages in rats with pressure overload. *Thorac Cardiovasc Surg*. 2013;61:718–725.
10. Doenst T, Pytel G, Schrepper A, Amorim P, Farber G, Shingu Y, Mohr FW, Schwarzer M. Decreased rates of substrate oxidation ex vivo predict the onset of heart failure and contractile dysfunction in rats with pressure overload. *Cardiovasc Res*. 2010;86:461–470.
11. Palmer JW, Tandler B, Hoppel CL. Biochemical properties of subsarcolemmal and interfibrillar mitochondria isolated from rat cardiac muscle. *J Biol Chem*. 1977;252:8731–8739.
12. Estabrook RW. Mitochondrial respiratory control and the polarographic measurement of ADP: O ratios. *Methods Enzymol*. 1967;10:41–47.
13. Fischer-Rasokat U, Beyersdorf F, Doenst T. Insulin addition after ischemia improves recovery of function equal to ischemic preconditioning in rat heart. *Basic Res Cardiol*. 2003;98:329–336.
14. Montalibet J, Skorey KI, Kennedy BP. Protein tyrosine phosphatase: enzymatic assays. *Methods*. 2005;35:2–8.
15. Nguyen TD, Shingu Y, Schwarzer M, Schrepper A, Doenst T. The E-wave deceleration rate E/DT outperforms the tissue Doppler-derived index E/e' in characterizing lung remodeling in heart failure with preserved ejection fraction. *PLoS One*. 2013;8:e82077.
16. Aubert G, Vega RB, Kelly DP. Perturbations in the gene regulatory pathways controlling mitochondrial energy production in the failing heart. *Biochim Biophys Acta*. 2013;1833:840–847.

17. Kannel WB, Hjortland M, Castelli WP. Role of diabetes in congestive heart failure: the Framingham study. *Am J Cardiol*. 1974;34:29–34.
18. Gray S, Kim JK. New insights into insulin resistance in the diabetic heart. *Trends Endocrinol Metab*. 2011;22:394–403.
19. Farese RV, Sajan MP, Standaert ML. Insulin-sensitive protein kinases (atypical protein kinase C and protein kinase B/Akt): actions and defects in obesity and type II diabetes. *Exp Biol Med (Maywood)*. 2005;230:593–605.
20. Copps KD, White MF. Regulation of insulin sensitivity by serine/threonine phosphorylation of insulin receptor substrate proteins IRS1 and IRS2. *Diabetologia*. 2012;55:2565–2582.
21. Qi Y, Xu Z, Zhu Q, Thomas C, Kumar R, Feng H, Dostal DE, White MF, Baker KM, Guo S. Myocardial loss of IRS1 and IRS2 causes heart failure and is controlled by p38alpha MAPK during insulin resistance. *Diabetes*. 2013;62:3887–3900.
22. Bouzakri K, Roques M, Gual P, Espinosa S, Guebre-Egziabher F, Riou JP, Laville M, Le Marchand-Brustel Y, Tanti JF, Vidal H. Reduced activation of phosphatidylinositol-3 kinase and increased serine 636 phosphorylation of insulin receptor substrate-1 in primary culture of skeletal muscle cells from patients with type 2 diabetes. *Diabetes*. 2003;52:1319–1325.
23. Luo M, Langlais P, Yi Z, Lefort N, De Filippis EA, Hwang H, Christ-Roberts CY, Mandarino LJ. Phosphorylation of human insulin receptor substrate-1 at Serine 629 plays a positive role in insulin signaling. *Endocrinology*. 2007;148:4895–4905.
24. Seely BL, Staubs PA, Reichart DR, Berhanu P, Milarski KL, Saltiel AR, Kusari J, Olefsky JM. Protein tyrosine phosphatase 1B interacts with the activated insulin receptor. *Diabetes*. 1996;45:1379–1385.
25. Shi K, Egawa K, Maegawa H, Nakamura T, Ugi S, Nishio Y, Kashiwagi A. Protein-tyrosine phosphatase 1B associates with insulin receptor and negatively regulates insulin signaling without receptor internalization. *J Biochem*. 2004;136:89–96.
26. Gomez E, Vercauteren M, Kurtz B, Ouvrard-Pascaud A, Mulder P, Henry JP, Besnier M, Waget A, Hooft Van Huijsduijnen R, Tremblay ML, Burcelin R, Thuillez C, Richard V. Reduction of heart failure by pharmacological inhibition or gene deletion of protein tyrosine phosphatase 1B. *J Mol Cell Cardiol*. 2012;52:1257–1264.
27. Gogiraju R, Schroeter MR, Bochenek ML, Hubert A, Munzel T, Hasenfuss G, Schafer K. Endothelial deletion of protein tyrosine phosphatase-1B protects against pressure overload-induced heart failure in mice. *Cardiovasc Res*. 2016;111:204–216.
28. Zhang L, Jaswal JS, Ussher JR, Sankaralingam S, Wagg C, Zaugg M, Lopaschuk GD. Cardiac insulin-resistance and decreased mitochondrial energy production precede the development of systolic heart failure after pressure-overload hypertrophy. *Circ Heart Fail*. 2013;6:1039–1048.
29. Turner N, Heilbronn LK. Is mitochondrial dysfunction a cause of insulin resistance? *Trends Endocrinol Metab*. 2008;19:324–330.
30. Hesselink MK, Schrauwen-Hinderling V, Schrauwen P. Skeletal muscle mitochondria as a target to prevent or treat type 2 diabetes mellitus. *Nat Rev Endocrinol*. 2016;12:633–645.
31. Stump CS, Short KR, Bigelow ML, Schimke JM, Nair KS. Effect of insulin on human skeletal muscle mitochondrial ATP production, protein synthesis, and mRNA transcripts. *Proc Natl Acad Sci USA*. 2003;100:7996–8001.
32. McKee EE, Grier BL. Insulin stimulates mitochondrial protein synthesis and respiration in isolated perfused rat heart. *Am J Physiol*. 1990;259:E413–E421.
33. Pagel-Langenickel I, Bao J, Joseph JJ, Schwartz DR, Mantell BS, Xu X, Raghavachari N, Sack MN. PGC-1alpha integrates insulin signaling, mitochondrial regulation, and bioenergetic function in skeletal muscle. *J Biol Chem*. 2008;283:22464–22472.
34. Boudina S, Bugger H, Sena S, O'Neill BT, Zaha VG, Ilkun O, Wright JJ, Mazumder PK, Palfreyman E, Tidwell TJ, Theobald H, Khalimonchuk O, Wayment B, Sheng X, Rodnick KJ, Centini R, Chen D, Litwin SE, Weimer BE, Abel ED. Contribution of impaired myocardial insulin signaling to mitochondrial dysfunction and oxidative stress in the heart. *Circulation*. 2009;119:1272–1283.
35. Heineke J, Molkentin JD. Regulation of cardiac hypertrophy by intracellular signalling pathways. *Nat Rev Mol Cell Biol*. 2006;7:589–600.
36. Li HH, Willis MS, Lockyer P, Miller N, McDonough H, Glass DJ, Patterson C. Atrogin-1 inhibits Akt-dependent cardiac hypertrophy in mice via ubiquitin-dependent coactivation of Forkhead proteins. *J Clin Invest*. 2007;117:3211–3223.
37. Wende AR, O'Neill BT, Bugger H, Riehle C, Tuinei J, Buchanan J, Tsushima K, Wang L, Caro P, Guo A, Sloan C, Kim BJ, Wang X, Pereira RO, McCrory MA, Nye BG, Benavides GA, Darley-Usmar VM, Shioi T, Weimer BC, Abel ED. Enhanced cardiac Akt/protein kinase B signaling contributes to pathological cardiac hypertrophy in part by impairing mitochondrial function via transcriptional repression of mitochondrion-targeted nuclear genes. *Mol Cell Biol*. 2015;35:831–846.
38. Goldstein BJ, Bittner-Kowalczyk A, White MF, Harbeck M. Tyrosine dephosphorylation and deactivation of insulin receptor substrate-1 by protein-tyrosine phosphatase 1B. Possible facilitation by the formation of a ternary complex with the Grb2 adaptor protein. *J Biol Chem*. 2000;275:4283–4289.

SUPPLEMENTAL MATERIAL

Figure S1. Changes in mRNA expression of genes regulating mitochondrial biogenesis.

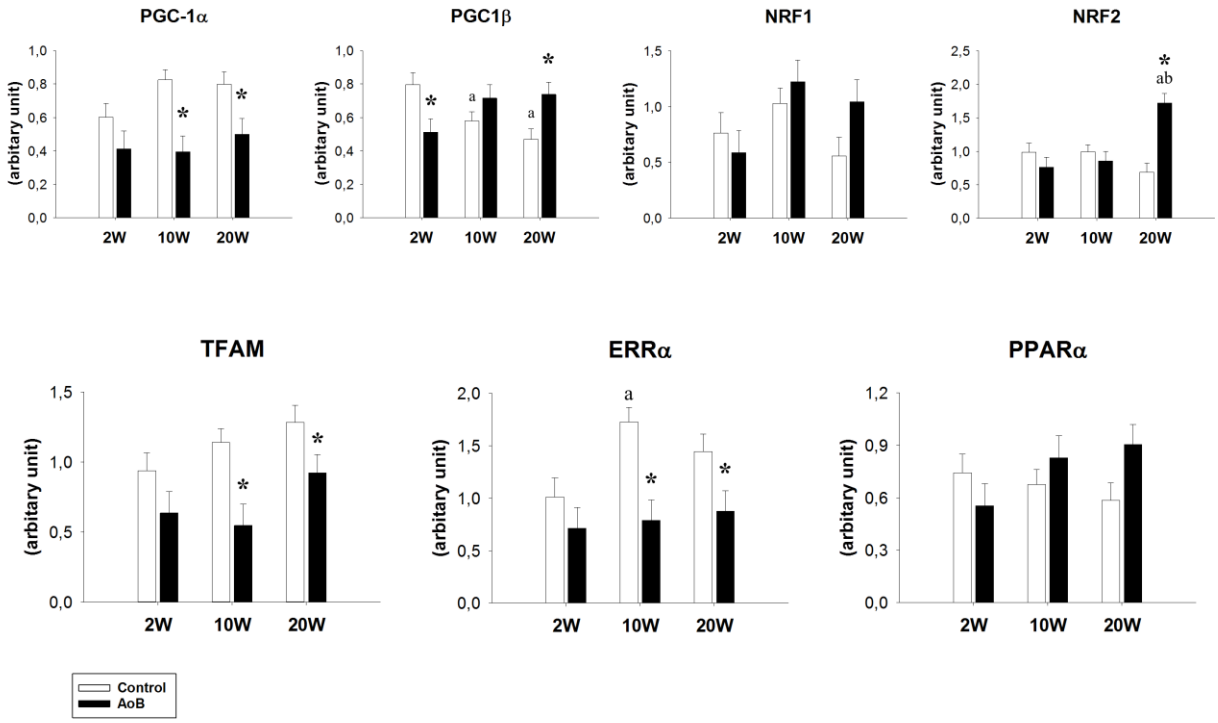

Data are Least Squares Mean ± SEM, n = 4 - 12. Statistical analysis: Two-way ANOVA with the Holm-Sidak method for pairwise comparisons. Significantly different vs. Control: *. Significantly different vs. 2 weeks: a, vs. 10 weeks: b (within Control or AoB)

Figure S2. Changes in mRNA expression of mitochondrial respiratory chain complex subunits.

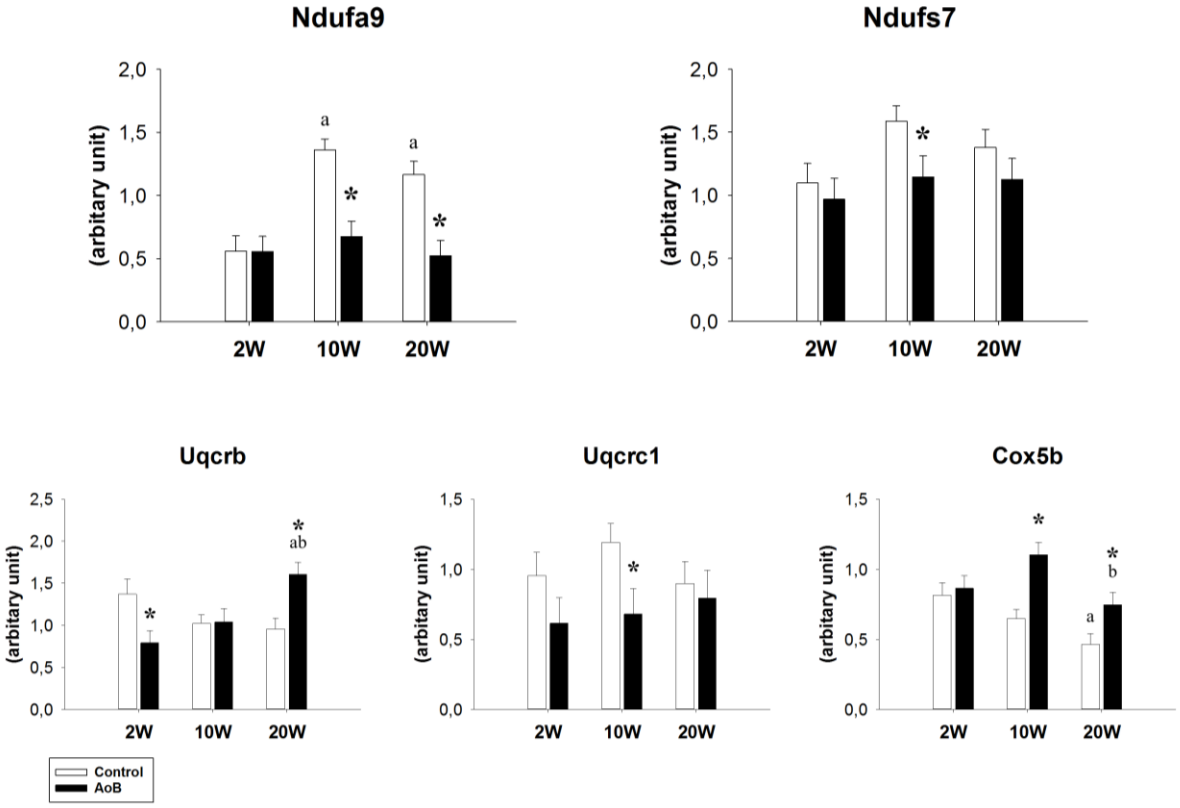

Data are Least Squares Mean ± SEM, n = 4 - 12. Statistical analysis: Two-way ANOVA with the Holm-Sidak method for pairwise comparisons. Significantly different vs. Control: *. Significantly different vs. 2 weeks: a, vs. 10 weeks: b (within Control or AoB)

Figure S3. Changes in Akt and IRS1 signaling at 2, 10 and 20 weeks after aortic banding.

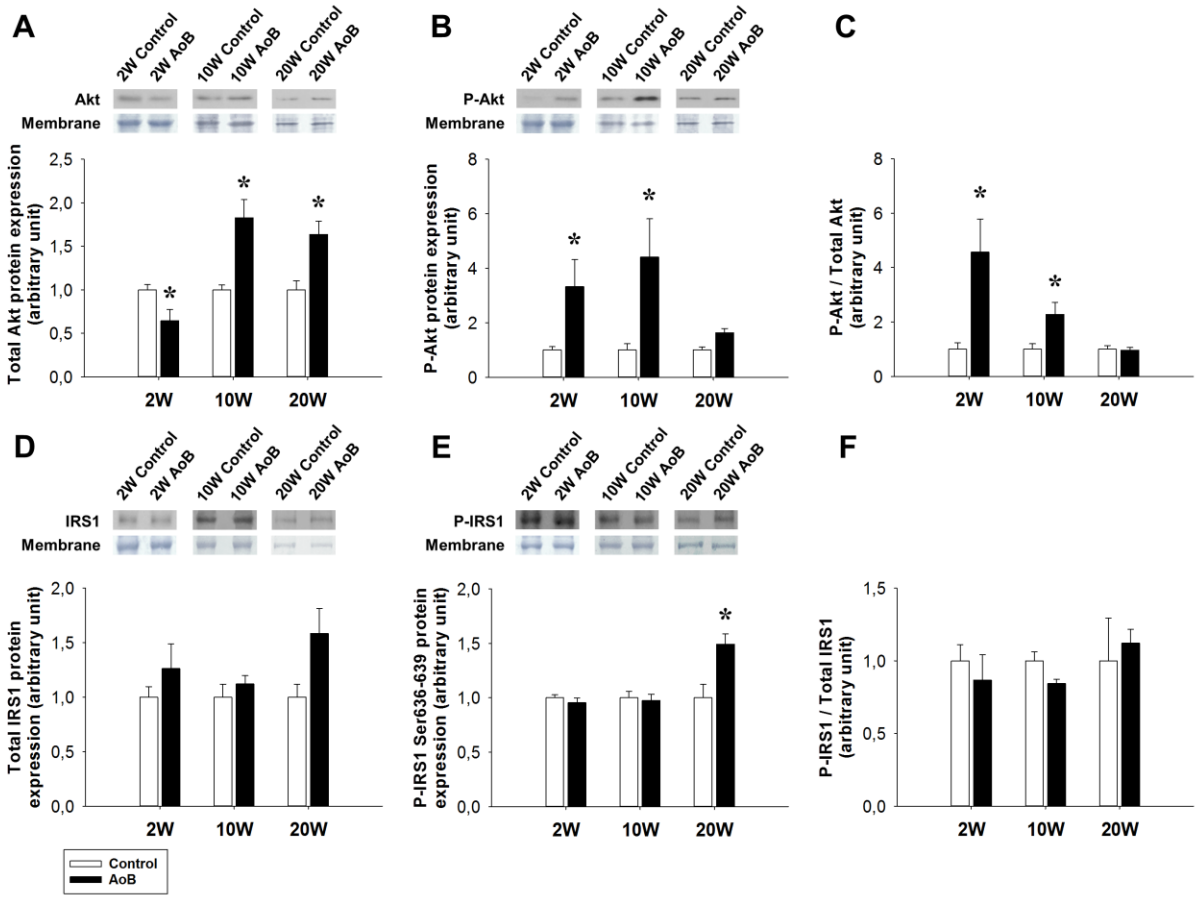

Total protein expression of Akt **(A)**. Protein expression of phosphorylated Akt **(B)**. Phosphorylation levels of Akt **(C)**. Total protein expression of IRS1 **(D)**. Protein expression of phosphorylated IRS1 at Ser636-639 **(E)**. Phosphorylation levels of IRS1 at Ser636-639 **(F)**. Data are Mean ± SEM, n = 4-7 per group. Statistical analysis: Student's t-test. Significantly different vs. Control: *